# In situ Raman spectroscopy measurements of $MgAl_2O_4$ spinel up to 1400 °C

SARAH P. SLOTZNICK AND SANG-HEON SHIM*

Department of Earth, Atmospheric, and Planetary Sciences, Massachusetts Institute of Technology, Massachusetts 02139, U.S.A.

## ABSTRACT

In-situ Raman measurements using a gated spectroscopy system revealed irreversible changes at 800–1000 °C in a natural red spinel (with 2 cation mol% Cr and 1 cation mol% Zn) and at 1100–1200 °C in a natural clear spinel (without Cr or Zn). Our observations of rapid broadening of a mode at 409 $cm^{-1}$ and the appearance of two weak modes at 210 and 520 $cm^{-1}$ at the transition temperature confirm the association of these features with cation disordering proposed by previous quench studies. Furthermore, we found that the frequencies of modes at 313 and 666 $cm^{-1}$ change at the transition temperature. The discontinuous frequency decrease of the mode at 313 $cm^{-1}$ and the increase in the frequency of the mode at 666 $cm^{-1}$ can be explained by the entrance of heavier Al atoms into the tetrahedral sites and the entrance of lighter Mg atoms into the octahedral sites, respectively. Our study demonstrates that in-situ Raman spectroscopy is a powerful tool for studying cation disordering in spinel-structured minerals at high temperature.

**Keywords:** Spinel, Raman spectroscopy, order-disorder transition, high temperature

## INTRODUCTION

Spinel-structured minerals, such as magnetite and ringwoodite, are important for understanding many geological and geophysical problems, such as paleomagnetism and mantle discontinuities. In ordered spinel ($MgAl_2O_4$), Mg and Al atoms are in the tetrahedral and the octahedral sites, respectively. Some Al atoms enter into the tetrahedral sites through an order-disorder transition at high temperature (Wood et al. 1986; Yamanaka and Takéuchi 1983; Peterson et al. 1991):

$$^{IV}Mg^{VI}Al_2O_4 \leftrightarrow {}^{IV}(Mg_{1-x}Al_x)^{VI}(Al_{2-x}Mg_x)O_4 \quad (1)$$

where the superscripts represent the coordination numbers of the cations and $x$ is the fraction of Al atoms in the tetrahedral sites, known as the inversion parameter. Spinels with $x = 0$ and $x = 1$ are called "normal" and "inverse," respectively.

Due to the similarities in the X-ray scattering cross sections between $Mg^{2+}$ and $Al^{3+}$, it has been challenging to directly determine the fraction of atoms in the octahedral and tetrahedral sites using X-ray diffraction (Yamanaka and Takéuchi 1983). In neutron diffraction, because Mg and Al atoms show much more contrast, direct characterization of cation disorder is possible (Peterson et al. 1991). However, neutron diffraction is not as readily accessible as other techniques.

Raman spectroscopy has been used to study cation disorder in spinel. In some $MgAl_2O_4$ spinels, more Raman modes have been observed than predicted by group theory (Fraas et al. 1973; O'Horo et al. 1973; Cynn et al. 1992). It has been suggested that most of these extra features are related to cation disorder (Cynn et al. 1992; Van Minh and Yang 2004; Chopelas and Hofmeister 1991). For example, an extra mode has been observed at 727 $cm^{-1}$ in synthetic and heat-treated natural spinels that are thought to be partially inverted (Cynn et al. 1992; Chopelas and Hofmeister 1991). In addition, asymmetric broadening of the most intense mode at 410 $cm^{-1}$, $E_g$, has been related to cation disorder as it is observed only in synthetic or heat-treated natural spinel (Cynn et al. 1992; Chopelas and Hofmeister 1991).

However, most Raman measurements for spinel to date have been conducted on temperature-quenched samples, although some in situ high-temperature Raman spectra were presented by Cynn et al. (1992). It has been thought that fast cooling after synthesis or heat treatment may help preserve cation disorder after quench (Cynn et al. 1992). However, previous diffraction (Yamanaka and Takéuchi 1983) and NMR (Wood et al. 1986) studies have suggested that cation disorder at high temperature is not fully preserved through the quench process.

One of the most important problems of using a conventional dispersive Raman technique for in situ high-temperature measurements has been the detection of intense thermal radiation from samples. This can be partially resolved by using short wavelength laser beams, such as 457.9 nm of an Ar-ion laser (e.g., Yashima et al. 1997). However, thermal radiation above 800 °C is too intense even at the near UV range for this technique to yield sufficient signal-to-background ratio. Pulsed lasers have been synchronized with gated detectors to study materials at extreme high temperature (Bernardez et al. 1992; Exarhos and Schaaf 1991; Fayette et al. 1994; Herchen and Cappelli 1991; McCarty 1990). The principle can be easily understood from the fact that photon counting statistics are determined by the Poisson distribution (Mulac et al. 1978), and acquisition time has an inverse relation with signal$^2$/background. Thus, by decreasing data acquisition time and accumulating many spectra, signal-to-background ratio can be enhanced.

* E-mail: sangshim@mit.edu

We have recently developed a gated spectroscopy system for in situ high-temperature measurements. We have demonstrated that compared with conventional dispersive Raman systems, the new gated Raman system improves the signal-to-background ratio by more than 4 orders of magnitude at 1400 °C (Shim et al. 2005). In this paper, we report an in situ high-temperature Raman study of two natural spinels with different chemical compositions up to 1400 °C using this technique.

## Experimental methods

We used two natural spinel samples from different locations. A clear spinel from Mongaragàla District, Sri Lanka (Harvard Mineralogical Museum no. 126100) is white with a bluish-purple tint. Chemical analysis shows that this spinel is almost pure $MgAl_2O_4$ except for a small amount of Fe (hereafter "clear spinel," Table 1). The other natural sample is from Moguk, Burma. This spinel is red (hereafter "red spinel"), and the chemical composition is very similar to the clear spinel except that it contains 2 cation mol% of Cr and 1 cation mol% of Zn (Table 1). Chromium is responsible for the red color (Burns 1993).

In order to identify spectral features that are related to cation disordering, we obtained a non-stoichiometric synthetic spinel ($MgO{\cdot}1.08Al_2O_3$) from Alfa Aesar. Because of excess Al, some Al should exist in the tetrahedral sites (Ishii et al. 1982). Therefore, the synthetic spinel should be at least partially inverted. Furthermore, Cynn et al. (1992) showed that even stoichiometric synthetic spinel is disordered due to fast cooling during synthesis. Chemical compositions of the samples were measured by energy-dispersive spectrometry using the electron microprobe facility at MIT.

During heating and cooling, a Raman spectrum was measured every 100 and 200 °C up to 1400 °C for the clear and red spinels, respectively, in the Linkam TS1500 heating stage (Fig. 1). Temperature was changed at a rate of 10 °C/min. Temperature was measured using a thermocouple attached directly to the microfurnace in the heating stage. Uncertainty in temperature is <5 °C. Once the target temperature was reached, temperature was fixed within ±1 °C for 20 min using the feedback system connected to a thermocouple reader and a power supply for Raman measurements. To prevent oxidation of heating elements and the samples, we passed pure Ar gas through the heating chamber throughout the runs. For the clear spinel, we conducted high-temperature measurements for the previously heated sample as well during heating and cooling (hereafter called "second heating" and "second cooling"), to investigate the effect of repeated heating on disordered spinel. After the high-temperature runs, the samples were left in the heating stage overnight to cool to room temperature.

Raman spectra were measured using a 526.5 nm line of a diode-pumped pulse laser (frequency doubled Nd:YLF) with a beam size of 20 μm on the sample (Fig. 1). A back-scattering geometry was used. The average power was set to 20 mW, which does not produce any visible damage on the surface of the samples. An intensified gated charge-coupled device (CCD) detector was synchronized with the pulse laser to achieve temporal filtering. Detailed description on our spectroscopy system will be provided elsewhere (Shim et al. in review). The gate width used was 20 ns and a total of 1 000 000 spectra were accumulated in each measurement. The spectrometer was calibrated using Ne spectral lines. The wavenumber calibration is better than 1 $cm^{-1}$. Spectral fitting was performed using a pseudo-Voigt profile shape function except for a mode at 409 $cm^{-1}$, which was fit to a split pseudo-Voigt profile shape function because of the asymmetry. This profile shape function allows us to measure widths of the left and right sides separately (Fig. 2). We then take the ratio between the left and right sides of the mode to parameterize the asymmetry: the asymmetry parameter is 1 for a symmetric peak and greater than 1 for an asymmetric peak with a broader left side.

**Table 1.** Chemical compositions of the natural spinel samples

| | Oxide % | | | Cation for 4O basis | |
|---|---|---|---|---|---|
| | Red spinel | Clear spinel | | Red spinel | Clear spinel |
| MgO | 27.15 | 27.33 | Mg | 0.98 | 0.97 |
| $Al_2O_3$ | 68.69 | 71.45 | Al | 1.97 | 2.00 |
| FeO | 1.17 | 1.08 | Fe | 0.02 | 0.02 |
| $Cr_2O_3$ | 0.95 | 0.01 | Cr | 0.02 | 0.00 |
| $SiO_2$ | 0.02 | 0.00 | Si | 0.00 | 0.00 |
| $TiO_2$ | 0.00 | 0.02 | Ti | 0.00 | 0.00 |
| MnO | 0.06 | 0.03 | Mn | 0.00 | 0.00 |
| CaO | 0.00 | 0.00 | Ca | 0.00 | 0.00 |
| NiO | 0.00 | 0.03 | Ni | 0.00 | 0.00 |
| ZnO | 0.58 | 0.05 | Zn | 0.01 | 0.00 |
| CoO | 0.11 | 0.00 | Co | 0.00 | 0.00 |
| Total | 98.74 | 100.00 | | 3.01 | 3.00 |

## Result

Group theory for the $Fd\bar{3}m$ space group predicts that a total of five modes are Raman active for spinel. At ambient conditions before heating, we observed a total of 4 modes for natural spinels (Figs. 3a and 3c; Table 2), which is consistent with previous Raman measurements (Fraas et al. 1973; Chopelas and Hofmeister 1991; Cynn et al. 1992). Good agreement in mode frequencies between the clear and red spinels is reasonable because of their similar compositions.

With an increase in temperature to 800 and 1100 °C in the red and clear spinels, respectively, we observe gradual decreases in mode frequencies and gradual increases in peak widths, which can be explained by the thermal effect (Figs. 3, 4, and 5). The $E_g$ peak shows very little asymmetry before heating (Fig. 6). We observe no significant increase in the asymmetry of the $E_g$ peak with heating (Figs. 6a and 6c).

The background counts of Raman spectra remain the same up to 1400 °C for the clear spinel (Fig. 3a), demonstrating the effectiveness of the gated spectrometry in reducing the detection of thermal radiation. Although the Raman spectrum of the red spinel at room temperature had a signal-to-background ratio similar

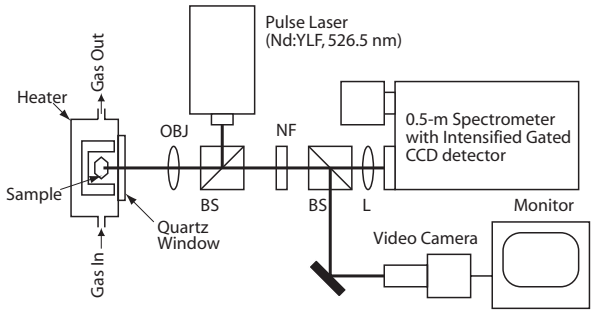


**Figure 1.** Schematic diagram of a nanosecond gated Raman spectroscopy system used in this study (OBJ = objective lens, NF = holographic notch filter, BS = beam splitter, L = lens).

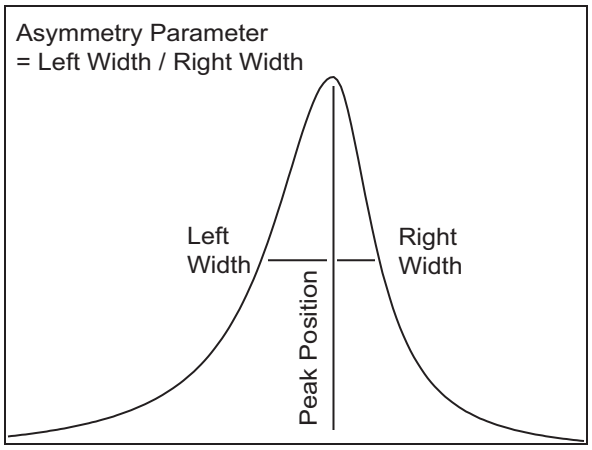


**Figure 2.** Split pseudo-Voigt profile shape function and the definition of asymmetry parameter used in this study.

**TABLE 2.** Frequencies ($cm^{-1}$) of Raman modes observed in different samples

| | This work | | | | | | Cynn* | | | Ishii† |
|---|---|---|---|---|---|---|---|---|---|---|
| | Clear Nat | | | Red Nat | | Syn | Pink Nat | | Syn | Syn |
| | 1st run | | 2nd run | | | | | | | |
| | Pre | Post | Post | Pre | Post | | Pre | Post | | |
| $N_1$ | | | 220 | | | 222 | | | | 223 |
| $T_{2g}(1)$ | 313 | 309 | 305 | 312 | 306 | 309 | 311 | 307 | 311 | 310 |
| $E_g$ | 408 | 411 | 409 | 407 | 409 | 410 | 409 | 407 | 409 | 410 |
| $T_{2g}(2)$ | 666 | 670 | 668 | 666 | 668 | 670 | 670 | 671 | 670 | 668 |
| $N_3$ | | 724 | 720 | | 720 | 720 | | 726 | 727 | 725 |
| $A_{1g}$ | 768 | 770 | 767 | 766 | 765 | 768 | 770 | 768 | 770 | 769 |

*Note:* Clear Nat = clear natural spinel, Red Nat = red natural spinel, Syn = synthetic spinel, Pink Nat = pink natural spinel, Pre = before heating, Post = after heating)
* Cynn et al. (1992).
† Non-stoichiometric spinel with a composition of $MgO{\cdot}3Al_2O_3$ (Ishii et al. 1982).

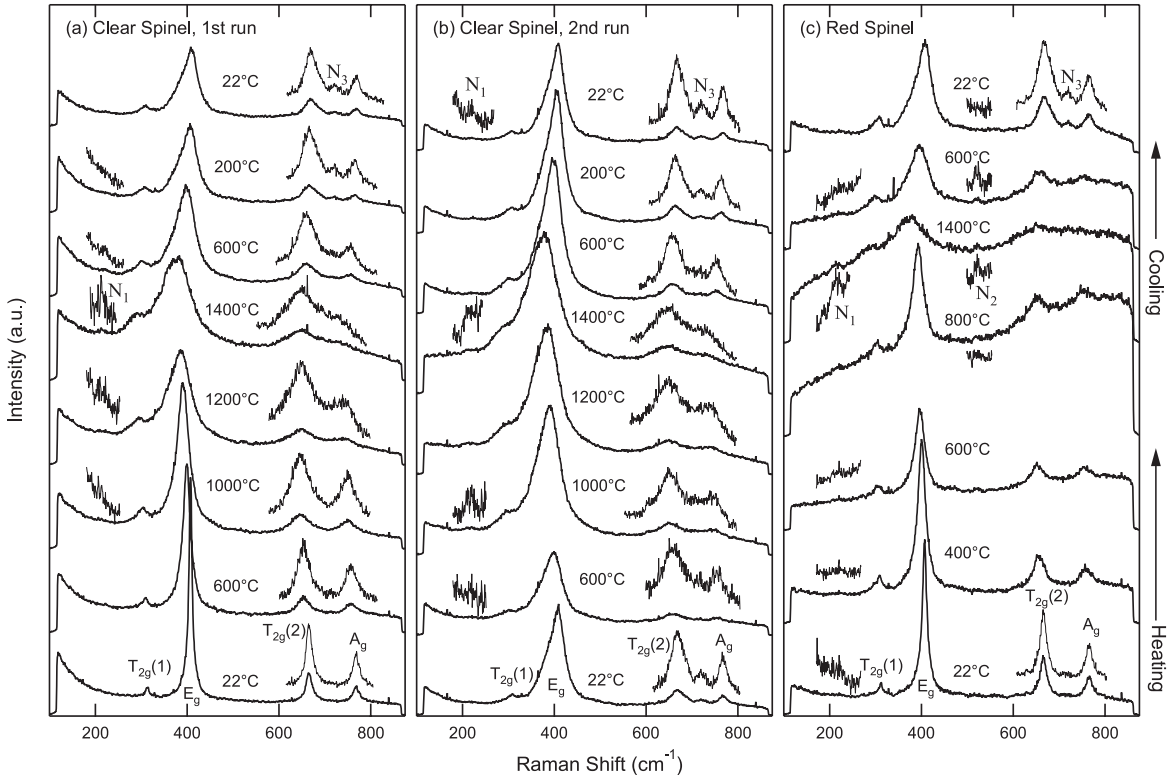


**FIGURE 3.** Raman spectra of the (**a**, **b**) clear and (**c**) red spinels measured at high temperatures. Raman spectra of the clear spinel during second heating cycle are shown in **b**. The insets show expanded views of weak spectral features. The modes appeared at high temperature are assigned tentatively ($N_1$–$N_3$) in the order of their frequencies.

to that of the clear spinel, the background increases drastically between 400 and 600 °C (Fig. 3c). This should not be a result of the increase in thermal radiation with temperature because our temporal filtering effectively suppresses the detection of thermal radiation for the clear spinel. From the color of the sample, we infer this large background increase due to temperature-dependent changes in the fluorescence of the red spinel. The sample shows a lower background when cooled below 600 °C, indicating that the background change is reversible (Fig. 3c).

A series of changes were observed between 800 and 1000 °C in the red spinel and between 1100 and 1200 °C in the clear spinel during heating. A weak mode appears at 213 $cm^{-1}$, $N_1$, in both natural spinels (Fig. 3). Another mode appears at 520 $cm^{-1}$, $N_2$, in the red spinel above 1200 °C. Three modes, $T_{2g}(1)$, $T_{2g}(2)$, and $A_g$, show changes in frequency at these temperature ranges: the frequency of the $T_{2g}(1)$ mode decreases discontinuously by 9 $cm^{-1}$ in the clear spinel and by 11 $cm^{-1}$ in the red spinel, whereas that of $T_{2g}(2)$ increases with temperature (Fig. 4). The frequency decrease in the $A_g$ mode is subtle. The width of the $E_g$ mode increases rapidly in these temperature ranges during heating (Figs. 5a and 5c). The left side width of the $E_g$ mode increases more rapidly than the right side in the clear spinel (Fig. 5a), resulting in an increase in the asymmetry of the peak (Fig. 6a). Although it is difficult to resolve a trend due to large data scatter, the asymmetry appears to increase above these temperature ranges, particularly in the clear spinel (Fig. 6a).

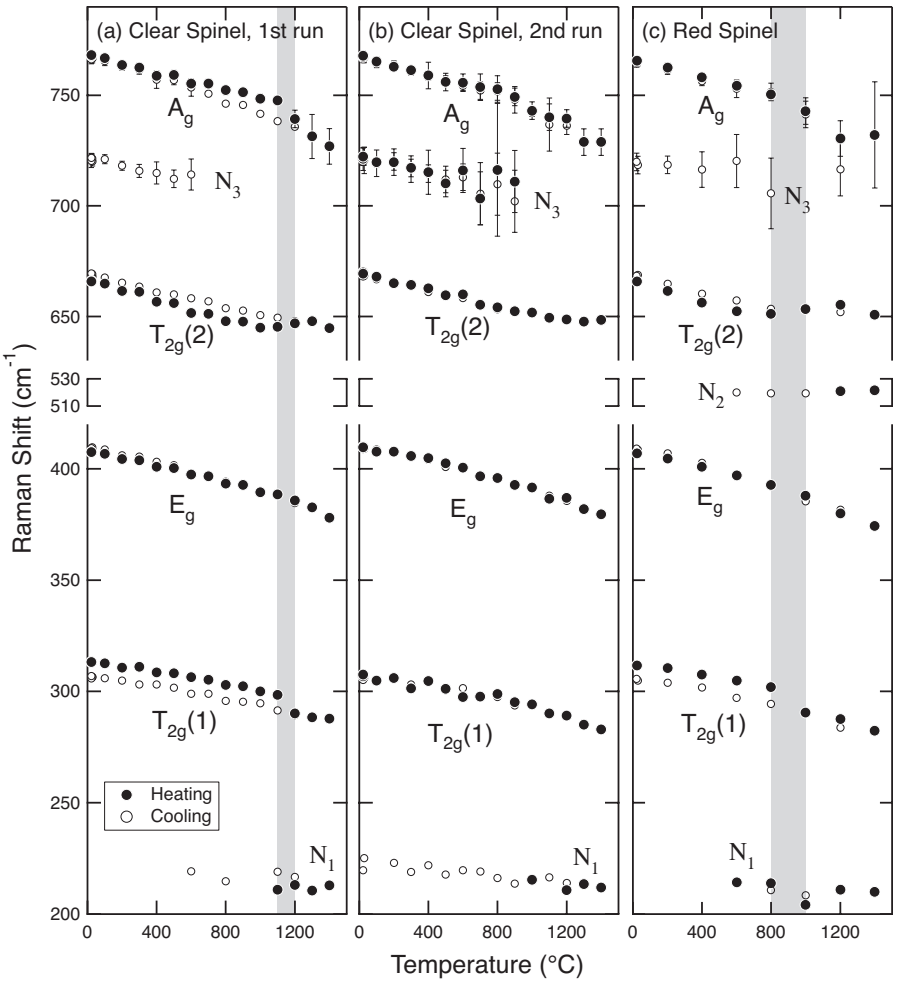


**FIGURE 4.** Frequency shifts of Raman modes with temperature. (**a**) First and (**b**) second runs for the clear spinel. (**c**) The red spinel. Temperature ranges for which we observed changes in the Raman spectrum are indicated by gray shading. Cooling data points (open circles) exist at the same temperatures as heating data points (solid circle). Some cooling data points completely overlap with heating data points. The error bars are 2σ estimated uncertainties. The size of the error bar is smaller than that of the symbol except for the $N_3$ and $A_g$ modes.

During cooling, the $N_1$ and $N_2$ peaks persist to 600 °C, but below this temperature they become difficult to resolve (Fig. 3). The frequencies of the $T_{2g}(1)$ and $T_{2g}(2)$ modes during cooling are systematically lower and higher, respectively, than during heating. This trend persists to room temperature (Fig. 4). This indicates that the changes at high temperature are irreversible. The frequency of the $A_g$ mode during cooling between 1100 and 700 °C is systematically lower than during heating in the clear spinel. However, the cooling trend merges into the heating trend below 700 °C.

A new mode, $N_3$, appears between the $T_{2g}(2)$ and $A_g$ modes at 600 °C during cooling (Fig. 3). Resolution of this peak is difficult down to 400 °C. However, spectral fitting improves when a peak, i.e., $N_3$, between the existing modes is introduced: without the $N_3$ peak, the fitted width of the $A_g$ peak is much larger than the widths of the other peaks, perhaps an artifact from accounting intensities of the weak $N_3$ peak at the lower frequency side. The $N_3$ peak remains in the spectrum when the sample is fully cooled to room temperature. This finding agrees with previous studies on quench samples showing that natural spinels heated above 800 °C have a new peak around 720 cm$^{-1}$ (Cynn et al. 1992; Van Minh and Yang 2004).

During cooling, the width of the $E_g$ mode decreases but at a much smaller rate than during heating, resulting in a much larger width after cooling (Figs. 5a and 5c). Moreover, the left-side width decreases much more slowly than the right-side width, leading to an increase in asymmetry with cooling (Fig. 6a and 6c). Also, the asymmetry of the $E_g$ mode remains after cooling to room temperature.

A subsequent heating ("second heating run") was conducted for the clear spinel (Fig. 3b). The abrupt changes observed in the first run were not found in the second run (Figs. 4b, 5b, and 6b). Also the widths and the mode frequencies are reversible (Figs. 4b and 5b). After the run, we found a decrease in the frequency of the $T_{2g}(1)$ mode by 4 cm$^{-1}$ compared with that measured after the first run (Table 2), which indicates a further increase in cation disorder by the subsequent heating.

We also conducted Raman measurements on a non-stoichiometric synthetic (i.e., partially disordered) spinel at ambient conditions (Fig. 7). The mode frequencies are in reasonable

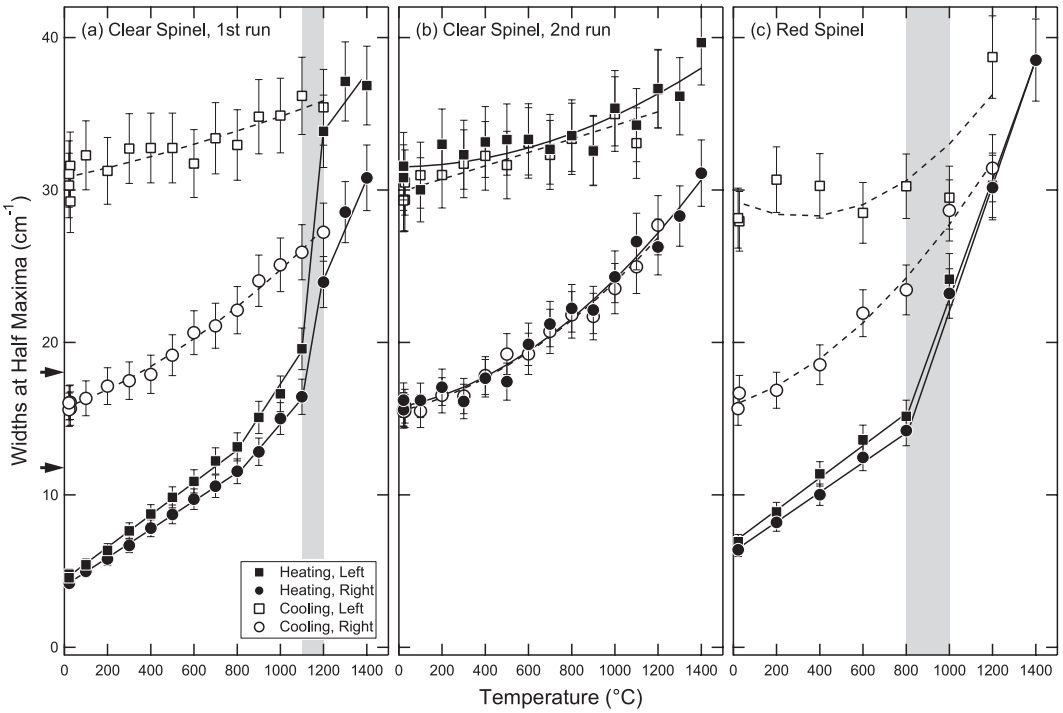


**FIGURE 5.** The left-and right-widths at half maximum for the $E_g$ mode at high temperatures. The widths in the non-stoichiometric synthetic spinel at room temperature are indicated by arrows. The error bars are 2σ estimated uncertainties. Other notations are the same as those in Figure 4.

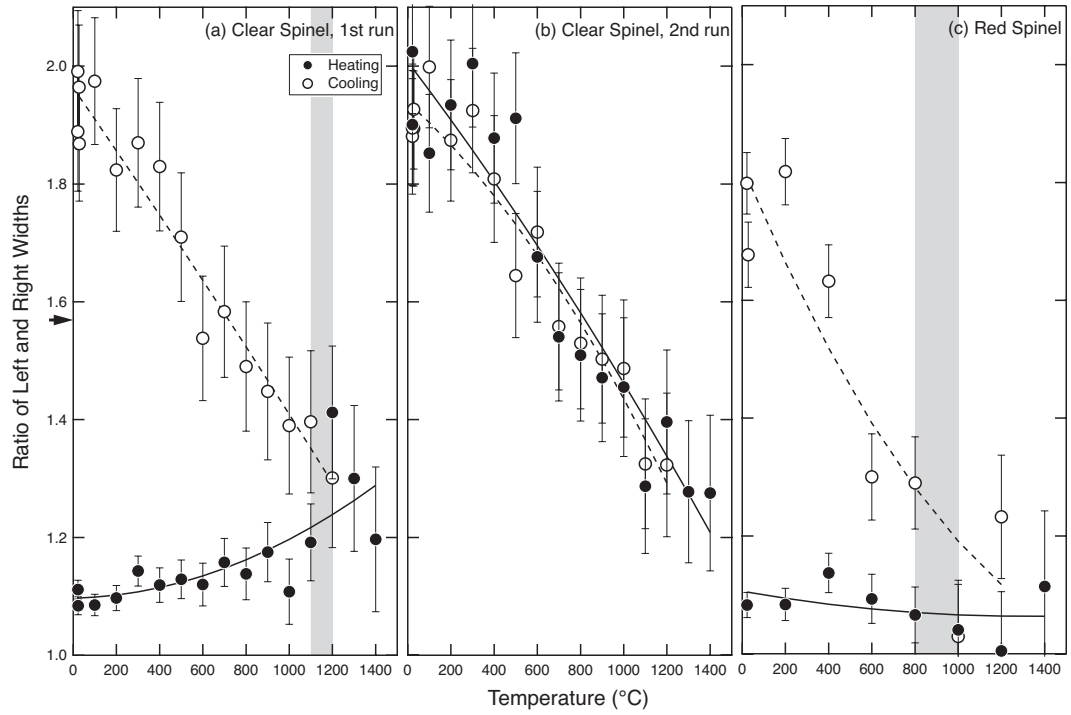


**FIGURE 6.** Ratio between the left-and right-side widths of the $E_g$ mode at high temperatures. The asymmetry in the non-stoichiometric synthetic spinel at room temperature is indicated by an arrow. The error bars are 2σ estimated uncertainties. Other notations are the same as those in Figure 4.

agreement with previous measurements on a non-stoichiometric spinel with a composition of $MgO \cdot 3Al_2O_3$ (Table 2) (Ishii et al. 1982). Comparison with this synthetic spinel allows us to identify features that are related to cation disorder. The spectrum of the synthetic spinel (Fig. 7) resembles those of the natural spinels after heating. The $N_3$ peak is observed in the synthetic spinel,

whereas it appears only after heating in the natural spinels. The $N_1$ peak was retained after the second heating of the clear spinel and it is observed in the synthetic spinel. The width of the $E_g$ mode is clearly larger in the synthetic spinel than it is in the natural spinels before heating. However, the width of this mode in the synthetic spinel is smaller than those of the natural spinels after heating. Also the asymmetry of the $E_g$ mode can be clearly seen in the spectrum of the synthetic spinel (Fig. 7). The asymmetry in the synthetic spinel is larger than that in the natural spinels before heating, but smaller than that after heating. Results of the non-stoichiometric synthetic spinel support that the appearance of $N_1$ and $N_3$, and the asymmetric broadening of the $E_g$ mode result from cation disorder. It is likely that the natural spinel after heating is more disordered than the non-stoichiometric synthetic spinel.

## Discussion

Through electron spin resonance, Schmocker and Waldner (1976) measured the inversion parameters of Cr-bearing synthetic and natural spinels. Depending on the impurities, two natural spinels showed different transition temperatures: 750–900 and 850–950 °C. Using NMR on quenched synthetic samples, Wood et al. (1986) reported 700–900 °C. This was subsequently supported by a neutron diffraction study (Peterson et al. 1991). These transition temperatures are in agreement with the temperatures at which we observed a series of changes in Raman spectra.

Our in situ Raman measurements show that the width of the $E_g$ mode increases rapidly near the transition temperature, confirming the suggestions of previous quench studies of the association of this change with cation disordering (Cynn et al. 1992). Our comparison with the non-stoichiometric synthetic spinel further supports this assignment.

Our high-temperature measurements also confirm that modes at 210 ($N_1$) and 520 ($N_2$) cm$^{-1}$ are related to cation disordering. The $N_2$ peak has been previously observed as a weak and broad mode in a natural spinel without heat treatment (Chopelas and Hofmeister 1991). This mode was assigned as a combination of low-frequency modes. However, we observe this peak only above the transition temperature during heating. This could indicate that the natural spinel used by Chopelas and Hofmeister (1991) was partially inverted. In addition, the use of a shorter wavelength laser line by Chopelas and Hofmeister (1991), 457.9 nm, could contribute to the difference. The $N_1$ mode has also been observed in non-stoichiometric synthetic spinels by Ishii et al. (1982) and in our study, suggesting that the mode is related to cation disorder.

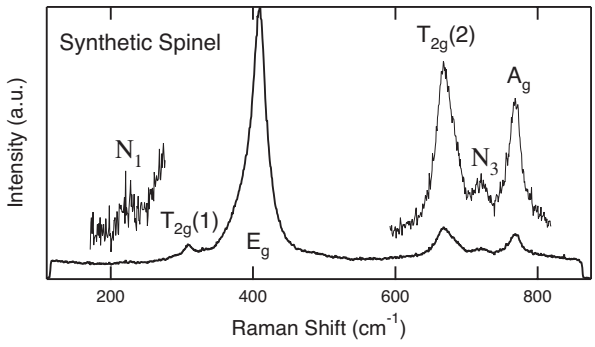


**Figure 7.** Raman spectrum of non-stoichiometric synthetic spinel ($MgO{\cdot}1.08Al_2O_3$) at ambient conditions. The insets show expanded views of weak spectral features.

The mode at 727 cm$^{-1}$ ($N_3$) has been related to cation disorder. Cynn et al. (1992) found that the $N_3$ mode may have the same symmetry as the $A_g$ mode and attributed the $N_3$ mode to the symmetric stretching (breathing) of the $AlO_4$ tetrahedra due to cation disorder. This argument was subsequently supported by a first-principles calculation (de Wijs et al. 2002). However, a later first-principles calculation by Lazzeri and Thilbaudeau (2006) proposed that the coupling of an inactive mode with the tetrahedral breathing mode is responsible for the observation of the $N_3$ mode. Regardless of mode assignment, both experiment and theory indicate that the mode is related to an order-disorder transition.

In our study, it is very difficult to resolve the $N_3$ mode at high temperature. The presence of this mode is only clear at temperatures below 600 °C. This is perhaps because the mode exists between more intense modes, i.e., $T_{2g}(2)$ and $A_g$. Resolution of the weak $N_3$ mode would be quite challenging particularly above the temperature where thermal broadening of the peaks is severe. Even at relatively low temperature, the resolution of the mode is only possible through spectral fitting. Therefore, we believe that limited observation for the $N_3$ mode in our study is due to the peak overlaps with adjacent modes.

Another feature that has been related to cation disordering in a previous quench study is the asymmetry of the $E_g$ mode (Cynn et al. 1992). No statistically significant change can be found on the asymmetry across the transition in our in situ study (Fig. 6). Because of thermal broadening overprinting the broadening from cation disordering, the asymmetry of the $E_g$ mode may not be a good criteria to detect disordering. However, based on the comparison with the Raman spectrum of the non-stoichiometric synthetic (partially inverted) spinel, it is likely that the asymmetry of the $E_g$ mode is associated with cation disorder.

One of the most important observations in this study is the frequency changes of the two $T_{2g}$ modes across the order-disorder transition. The $T_{2g}(1)$ mode has been assigned to the translation of Mg atoms in the tetrahedral sites, which is further supported by comparison with Raman spectrum of gahnite ($ZnAl_2O_4$) (Chopelas and Hofmeister 1991). The discontinuous negative shift of the $T_{2g}(1)$ frequency can be explained by the entrance of heavier Al atoms into the tetrahedral sites. The negative frequency shift of the $T_{2g}(1)$ mode rather than the appearance of a new mode indicates that vibrations of the $MgO_4$ and $AlO_4$ tetrahedra may still couple strongly with each other, so that treatment of them as separate isolated vibrational units is inappropriate in $MgAl_2O_4$ spinel.

Two more modes show frequency shifts at the transition temperature, i.e., $T_{2g}(2)$ and $A_g$. Although it is likely that the $N_3$ mode exists as a broad and weak peak, we found no statistical significance of introducing a peak between the $T_{2g}(2)$ and $A_g$ modes in spectral fitting for the data measured above 600 °C. Thus, we fit the spectra with two peaks. This would increase unfitted intensities between the $T_{2g}(2)$ and $A_g$ modes and would force the weak $A_g$ mode to fit the unfitted intensity ($N_3$) as well.

However, as shown in Figure 3, because the $T_{2g}(2)$ mode has high intensity and a well-defined peak shape up to our maximum temperature, it is unlikely that the spectral fitting can be severely affected by the unresolved $N_3$ peak. Therefore, we believe that

the positive shift of the $T_{2g}(2)$ mode is reliable. Chopelas and Hofmeister (1991) assigned the $T_{2g}(2)$ mode to an octahedral bending motion. The positive frequency shift across the transition temperature could be explained by entrance of lighter Mg atoms into the octahedral sites.

The frequency shifts of the two $T_{2g}$ modes are preserved during cooling with slight decreases (Table 2): $\Delta\nu = -3\sim6$ cm$^{-1}$ for the $T_{2g}(1)$ mode (−9 cm$^{-1}$ at the transition), and $\Delta\nu = +2\sim3$ cm$^{-1}$ for the $T_{2g}(2)$ mode (+11 cm$^{-1}$ at the transition). The slight decrease may indicate re-ordering of cations during cooling. The frequency differences at room temperature are close to the precision of wavenumber in typical Raman measurements, which perhaps explains why these frequency changes were not regarded as statistically significant in previous quench studies. However, systematic persistence of the differences for a wide temperature range in our in situ measurements supports the interpretation that the frequency changes are inherent to structural changes in spinel. The fact that the frequency of $T_{2g}(1)$ measured before and after heating by Cynn et al. (1992) shows a change by $\Delta\nu = -4$ cm$^{-1}$ (Table 2) supports the findings of the present work.

Although the transition temperature is in reasonable agreement with previous studies, the clear spinel shows the transition at higher temperature by 200–300 °C than the red spinel. The high-transition temperature could be related to the near end-member chemical composition of the clear spinel. It would be quite surprising if low concentration (≤2 mol%) impurities (such as Cr and Zn) can result in such a large difference in transition temperature. However, as pointed out in previous studies (Schmocker and Waldner 1976; Wood et al. 1986; Yamanaka and Takéuchi 1983), because many other factors can influence the transition temperature, measurements for spinel samples with known thermal history will be important to further investigate the role of impurities for the order-disorder transition.

It has been predicted that Mg-Si disorder in silicate spinel [ringwoodite ($\gamma$-$Mg_2SiO_4$)], could result in changes in the Clapeyron slopes of related phase transitions in the transition zone (Jackson et al. 1974; Navrotsky 1977) and the elastic properties (Li et al. 2007). Because the contrast in X-ray scattering cross sections between $Mg^{2+}$ and $Si^{4+}$ is very small, i.e., they both have 10 electrons, Mg-Si disorder has been only studied for quenched samples using the bond lengths between cations and anions (Hazen et al. 1993). As emphasized by Hazen and Yang (1999), cations can be re-ordered during temperature quench. Therefore, it is important to carry out in situ measurements for Mg-Si disorder in silicate spinels. Our measurements demonstrate that in situ Raman spectroscopy can be a powerful tool to study cation disordering in spinel-structured materials. This opens up an opportunity to study Mg-Si disorder in ringwoodite.

## Acknowledgments

We thank R. Hazen and B. Wopenka for their reviews. Discussions with T. Grove inspired us to conduct this measurement. C. Francis at Mineralogical Museum of Harvard University provided the clear natural spinel. E. Medard assisted cutting the natural spinel samples. Construction of the pulsed laser Raman system was supported by NSF (EAR0337156). Raman measurements were supported by NSF (EAR0337005). S. Slotznick is supported by the Leslie C. Patron Undergraduate Research Opportunity Program Fund.

## References cited

Bernardez, L., McCarty, K.F., and Yang, N. (1992) In situ Raman spectroscopy of diamond during growth in a hot filament reactor. Journal of Applied Physics, 72, 2001–2005.

Burns, R.G. (1993) Mineralogical Applications of Crystal Field Theory. Cambridge University Press, New York.

Chopelas, A. and Hofmeister, A.M. (1991) Vibrational spectroscopy of aluminate spinels at 1 atm and of $MgAl_2O_4$ to over 200-kbar. Physics and Chemistry of Minerals, 18, 279–293.

Cynn, H., Sharma, S.K., Cooney, T.F., and Nicol, M. (1992) High-temperature Raman investigation of order-disorder behavior in the $MgAl_2O_4$ spinel. Physical Review B, 45, 500–502.

de Wijs, G.A., Fang, C.M., Kresse, G., and de With, G. (2002) First-principles calculation of the phonon spectrum of $MgAl_2O_4$ spinel. Physical Review B, 65, 094305.

Exarhos, G.J. and Schaaf, J.W. (1991) Raman scattering from boron nitride coatings at high temperatures. Journal of Applied Physics, 69, 2543–2548.

Fayette, L., Marcus, B., Mermoux, M., Rosman, N., Abello, L., and Lucazeau, G. (1994) In situ Raman spectroscopy during diamond growth in a microwave plasma reactor. Journal of Applied Physics, 76, 1604–1608.

Fraas, L.M., Moore, J.E., and Salzberg, J.B. (1973) Raman characterization studies of synthetic and natural $MgAl_2O_4$ crystals. Journal of Chemistry and Physics, 58, 3585–3592.

Hazen, R.M. and Yang, H. (1999) Effects of cation substitution and order-disorder on *P-V-T* equations of state of cubic spinels. American Mineralogist, 84, 1956–1960.

Hazen, R.M., Downs, R.T., Finger, L.W., and Ko, J.D. (1993) Crystal-chemistry of ferromagnesian silicate spinels—evidence for Mg-Si disorder. American Mineralogist, 78, 1320–1323.

Herchen, H. and Cappelli, M.A. (1991) First-order Raman spectrum of diamond at high temperatures. Physical Review B, 43, 11740–11744.

Ishii, M., Hiraishi, J., and Yamanaka, T. (1982) Structure and lattice vibrations of Mg-Al spinel solid solution. Physics and Chemistry of Minerals, 8, 64–68.

Jackson, I.N.S., Liebermann, R.C., and Ringwood, A.E. (1974) Disproportionation of spinels to mixed oxides: Significance of cation configuration and implications for the mantle. Earth and Planetary Science Letters, 24, 203–208.

Lazzeri, M. and Thilbaudeau, P. (2006) Ab initio Raman spectrum of the normal and disordered $MgAl_2O_4$ spinel. Physical Review B, 74, 140301.

Li, L., Carrez, P., and Weidner, D. (2007) Effect of cation ordering and pressure on spinel elasticity by ab initio simulation. American Mineralogist, 92, 174–178.

McCarty, K.F. (1990) Investigations of materials at high temperatures using Raman spectroscopy. High Temperature Science, 26, 19–30.

Mulac, A.J., Flower, W.L., Hill, R.A., and Aeschliman, D.P. (1978) Pulsed spontaneous Raman scattering technique for luminous environments. Applied Optics, 17, 2695–2699.

Navrotsky, A. (1977) Calculation of effect of cation disorder on silicate spinel phase boundaries. Earth and Planetary Science Letters, 33, 437–442.

O'Horo, M.P., Frisillo, A.L., and White, W.B. (1973) Lattice vibrations of $MgAl_2O_4$ spinel. Journal of Physics and Chemistry of Solids, 34, 23–28.

Peterson, R.C., Lager, G.A., and Hitterman, R.L. (1991) A time-of-flight neutron powder diffraction study of $MgAl_2O_4$ at temperatures up to 1273 K. American Mineralogist, 76, 1455–1458.

Schmocker, U. and Waldner, F. (1976) The inversion parameter with respect to the space group of $MgAl_2O_4$ spinels. Journal of Physics C Solid State Physics, 9, L235–L237.

Shim, S.-H., Lamm, R., Rekhi, S., Catalli, K., Santill'an, J., and Lundin, S. (2005) New micro-Raman spectroscopy systems for high-temperature studies in the diamond anvil cell. In Eos Transaction Fall Meeting Supplement, volume 86, p. MR13B-02, American Geophysical Union.

Van Minh, N. and Yang, I.-S. (2004) A Raman study of cation-disorder transition temperature of natural $MgAl_2O_4$ spinel. Vibrational Spectroscopy, 35, 93–96.

Wood, B.J., Kirkpatrick, R.J., and Montez, B. (1986) Order-disorder phenomena in $MgAl_2O_4$ spinel. American Mineralogist, 71, 999–1006.

Yamanaka, T. and Takéuchi, Y. (1983) Order-disorder transition in $MgAl_2O_4$ spinel at high temperatures up to 1700 °C. Zeitschrift für Kristallographie, 165, 65–78.

Yashima, M., Kakihana, M., Shimidzu, R., Fujimori, H., and Yoshimura, M. (1997) Ultraviolet 363.8-nm Raman spectroscopy system for in situ measurements at high temperatures. Applied Spectroscopy, 51, 1224–1228.

Manuscript received May 3, 2007
Manuscript accepted September 27, 2007
Manuscript handled by Brigitte Wopenka